PROTEINS: Structure, Function, and Genetics 50:213–221 (2003)

Interaction of *E. coli* Outer-Membrane Protein A with Sugars on the Receptors of the Brain Microvascular Endothelial Cells

Deepshikha Datta,[1] Nagarajan Vaidehi,[1] Wely B. Floriano,[1] Kwang S. Kim,[2] Nemani V. Prasadarao,[3] and William A. Goddard III[1]*

[1]*Materials and Process Simulation Center (MC 139-74), California Institute of Technology, Pasadena, California*
[2]*Department of Pediatrics, Johns Hopkins University, Baltimore, Maryland*
[3]*Division of Infectious Diseases, Children's Hospital of Los Angeles and Keck School of Medicine University of Southern California, Los Angeles, California*

ABSTRACT ***Esherichia coli,* the most common gram-negative bacteria, can penetrate the brain microvascular endothelial cells (BMECs) during the neonatal period to cause meningitis with significant morbidity and mortality. Experimental studies have shown that outer-membrane protein A (OmpA) of *E. coli* plays a key role in the initial steps of the invasion process by binding to specific sugar moieties present on the glycoproteins of BMEC. These experiments also show that polymers of chitobiose (GlcNAcβ1-4GlcNAc) block the invasion, while epitopes substituted with the L-fucosyl group do not. We used HierDock computational technique that consists of a hierarchy of coarse grain docking method with molecular dynamics (MD) to predict the binding sites and energies of interactions of GlcNAcβ1-4GlcNAc and other sugars with OmpA. The results suggest two important binding sites for the interaction of carbohydrate epitopes of BMEC glycoproteins to OmpA. We identify one site as the binding pocket for chitobiose (GlcNAcβ1-4GlcNAc) in OmpA, while the second region (including loops 1 and 2) may be important for recognition of specific sugars. We find that the site involving loops 1 and 2 has relative binding energies that correlate well with experimental observations. This theoretical study elucidates the interaction sites of chitobiose with OmpA and the binding site predictions made in this article are testable either by mutation studies or invasion assays. These results can be further extended in suggesting possible peptide antagonists and drug design for therapeutic strategies. Proteins 2003;50:213–221.** © 2002 Wiley-Liss, Inc.

Key words: outer-membrane protein A; *E. coli* meningitis; chitobiose; binding site predictions

INTRODUCTION

Escherichia coli, a common gram-negative bacterium, causes meningitis during the neonatal period.[1,2] The morbidity and mortality associated with this disease has remained significant with case fatality rates ranging from 15–40% of the infected neonates while ≈50% of the survivors sustain neurological sequelae.[1,3] Incomplete understanding of the pathogenesis and pathophysiology of *E. coli* meningitis has hampered the development of new therapeutic avenues, thus contributing to the high morbidity and mortality. For example, *E. coli* meningitis develops as a result of hematogenous spread. However, it is not clear how the circulating *E. coli* traverses across the blood–brain barrier, which contains a single cell lining of the brain microvascular endothelial cells (BMECs). Several cell surface structures (such as S-fimbriae) present in *E. coli* are involved in the pathogenesis of *E. coli* meningitis. However, one of the more important steps involves the interaction of outer-membrane protein A (OmpA) with the BMEC. Prasadarao et al.[4] showed that the expression of OmpA enhances the *E. coli* invasion of BMEC. Thus, $OmpA^+$ *E. coli* strains invade BMEC with 50- to 100-fold higher frequency than $OmpA^-$ *E. coli* strains.[4] Moreover, OmpA interacts with a 95-kDa BMEC glycoprotein, Ecgp for *E. coli* invasion, which is specifically expressed in endothelial cells of brain origin but not of systemic origin (N.V. Prasadarao private communication). To examine the specificity of interaction of the sugar moieties on Ecgp, the BMEC was treated with wheat germ agglutinin (WGA), which blocked *E. coli* invasion.[5] Because WGA is specific to binding of GlcNAcβ1-4GlcNAc epitopes, it was concluded that WGA binds to GlcNAcβ1-4GlcNAc epitopes on the glycoprotein on BMEC, thus preventing invasion. However, treatment of BMEC with WGA does *not* block the interaction of S-fimbriae (specific for NeuAc2,3-galactose epitopes) binding to BMEC. This suggests that the inhibition is specific to chitobiose and not a mere steric hindrance by lectin. Other lectins such as ConA (specific to mannose) and AAL (specific to NeuAc2,3-galactose) did not show such blocking activity.[6] In addition, during invasion $OmpA^+$ *E. coli* induces actin filament rearrangement in

Grant sponsor: NIH/NICHD; Grant sponsor: NIH; Grant number: R29AI40567 (to NVP)

*Correspondence to: William A. Goddard III, California Institute of Technology—MSC, Beckman Institute (139-74), Pasadena, CA 91125. E-mail: wag@wag.caltech.edu

Received 7 August 2001; Accepted 28 June 2002

BMEC, but this rearrangement is blocked significantly by both chitobiose and wheat germ agglutinin.[7] On the other hand, OmpA$^-$ *E. coli* did not exhibit any effect on actin rearrangement.[7] Moreover, chitobiose–sepharose chromatography shows binding of OmpA to chitobiose, suggesting that the observed inhibition is due to the direct interaction of OmpA with GlcNAcβ1-4GlcNAc epitopes.

Prasadarao et al. have further shown that masking of OmpA with GlcNAcβ1-4GlcNAc epitopes significantly reduces the incidence of meningitis in a newborn rat model of hematogenous meningitis, suggesting the biologic relevance of this interaction.[6] They tested simple disaccharides such as chitobiose, lactose, cellobiose, and fucosyl-substituted chitobiose for invasion assays and showed clearly that chitobiose blocks the invasion of BMEC by *E. coli* while lactose, cellobiose, and fucosyl-substituted chitobiose do not.

Although the GlcNAcβ1-4GlcNAc epitopes are universally present on many N-linked glycoproteins, studies by Prasadarao et al. indicate clearly that OmpA interaction with GlcNAcβ1-4GlcNAc epitopes on Ecgp is crucial for the establishment of the disease. It has been demonstrated[8–10] that the same sugar or amino acid present on different proteins can contribute to specificity of the pathogen.[5,6] For example, enteropathogenic *E. coli* binding to epithelial cells depends on type 1 fimbriae, which is specific to the mannose residue and can be blocked by mannose sugar.[6] However, the same strain does not bind to BMEC efficiently even though BMEC contain mannose residues. This suggests that either the protein sequence and conformation around the GlcNacβ1-4GlcNAc epitopes in Ecgp or the density of the carbohydrate-bearing proteins on BMEC differ from that of epithelial cells and might depend on the microenvironment of the cells. Thus, these extensive biochemical studies provide evidence that OmpA interacts with chitobiose and that this interaction could be important in the initial steps of the *E. coli* pathogenesis.

Experiments have also shown that two short synthetic peptides (the hexamer, Asn27-Gly32, and the pentamer, Gly65-Asn69) generated from the N-terminal amino acid sequence of OmpA exhibit significant inhibition of OmpA-contributed *E. coli* invasion of BMEC.[5] These results indicate that the interaction of amino acid residues in loops 1 and 2 of the OmpA interact with GlcNAcβ1-4GlcNAc epitopes for *E. coli* invasion of BMEC.

On the other hand, OmpA-mediated *E. coli* invasion was not observed with systemic endothelial cells such as HUVEC.[5] Further studies on systemic endothelial cells revealed that the majority of GlcNAcβ1-4GlcNAc epitopes are substituted with L-fucose, thus possibly blocking the interaction with OmpA for *E. coli* invasion.

These findings strongly implicate OmpA as a major microbial structure necessary for the neurotropic nature of *E. coli* to invade BMEC, an important event in the pathogenesis of *E. coli* meningitis. Blocking of the OmpA binding site by small molecules is a potential strategy to prevent the penetration of *E. coli* into the central nervous system. Thus, to lay the groundwork for rational drug design, we initiated studies of the molecular-level interactions of OmpA with chitobiose and other disaccharides already tested experimentally.

OmpA is a highly conserved outer-membrane protein of *E. coli* with a molecular weight of ≈35 kDa (325 amino acids) containing 8 transmembrane domains and 4 extracellular loops. The crystal structure of the N-terminal 1–171 residues in the transmembrane domain of OmpA has been solved[11] to a resolution of 2.5 Å and further refined to 1.65 Å.[12] The crystal structure consists of a regular eight-stranded β-barrel with large water-filled cavities but does not form a pore. The barrel is exceptionally long with an average length of 13 residues. The barrel interior is polar with salt bridge networks that form a barrier for passage of water or ions. Nevertheless, it contains water-filled cavities that could serve as interaction sites with other proteins. The four extracellular loops are mobile and not well defined in the crystal. The high-resolution structure of OmpA[12] is better resolved in the transmembrane regions, but there are several missing residues in other regions. Hence, our study uses the 2.5-Å structure [Protein Data Bank (PDB) ID: 1bxw] because this was complete.[11] The hexamer, Asn27-Gly32, and pentamer, Gly65-Asn69, tested for inhibition of *E. coli* invasion are present in extracellular loops L1 and L2.

In this article, we use the HierDock first principles simulation procedure[13] to predict the binding site of chitobiose in OmpA. The HierDock procedure finds two important interaction sites on OmpA favorable to chitobiose. Substitution of the fucosyl group on chitobiose makes the epitope unfavorable for binding to OmpA, providing an explanation for why *E. coli* does not invade the systemic endothelial cells.

METHODS AND VALIDATION

To obtain an accurate description of the binding of small molecules to a protein requires an accurate description of the forces between them plus an accurate description of the changes in solvation that accompany binding. Also required is a comprehensive conformation search over the potential binding sites while considering all plausible conformation changes in the ligand and protein. The best computational methods are believed to provide reasonably accurate predictions of relative binding energies[14–16]; however, for cases where the binding site is not known it is not practical to use these most accurate methods at every possible site. Thus, we developed the HierDock hierarchical strategy, which starts with a coarse grain search (fast but not too accurate) over the full protein to identify the best sites for finer-grain studies, followed by a succession of increasingly accurate but increasingly costly studies that ultimately include an accurate description of solvation and fully flexible protein and ligand. HierDock has previously been applied successfully to predict the binding of nonnatural amino acids to phenylalanyl *t*-RNA synthetase[17] and the affinity of odorants to the mammalian olfactory receptor,[13] a membrane-bound protein.

HierDock uses a coarse grain docking procedure, currently DOCK4.0,[18] to select an ensemble of conformations over which to do a hierarchy of more accurate (fine-grain)

molecular dynamics (MD) annealing[19] to optimize the ligand in the various potential binding sites. The MD calculations use an all-atom force field (FF) with continuum solvation calculations of the energies and forces arising from solvation for both the ligand and the protein receptor.[20,21] The Poisson–Boltzmann (PB) description[20] leads to accurate energies and forces to describe the solvent effects on the energies and structure of small molecules. However, PB is too slow for MD. Consequently, we use the surface-generalized Born (SGB) method,[21] which leads to a reasonably accurate description of the solvent effects at considerably less cost. We found that the SGB method leads to results as accurate as the PB method in describing the electrostatic response of the solvent.[22] These solvation methods have been used in our calculations of scoring functions.

FF Validation Studies

Critical elements of the HierDock protocol are the hierarchical sequence of conformational searching, the accuracy of the FF, and the inclusion of solvation in the calculating structures and binding energy.

We use the DREIDING FF[23] with CHARMM[24] charges for the protein and charge equilibration[25] charges for the carbohydrate/sugar ligands. This approach has been used previously to study the binding of chitin (a polysaccharide) to family 18 and 19 chitinases.[26,27] Simulated annealing dynamics were reported[26] for hexaNAG substrate binding to family 18 chitinase. The root mean square (RMS) in coordinates for all atoms in the binding site was 2.13 Å, which is within the crystal resolution.

In another study,[28] we predicted the structure of sugars bound to proteins and compared to cocrystal structures available for these complexes. Here, we performed calculations for the binding of L-arabinose and D-fucose to the L-arabinose binding protein (PDB ID 1abe). Starting with the crystal structure (1abe), the ligands were removed from the binding pocket and using the HierDock protocol (DREIDING FF) we docked L-arabinose and D-fucose to the 1abe structure. The predicted structures of the protein–ligand complexes are in good agreement with the crystal structures (coordinate RMS error of 0.4 Å compared to the crystal structure of L-arabinose in L-arabinose binding protein, 1abe). The coordinate RMS error for D-fucose binding to L-arabinose binding protein is 1.4 Å compared to the corresponding crystal structure (1abf). Using a single target protein as a starting point, we predicted the cocrystal structure of both L-arabinose and D-fucose binding to L-arabinose binding protein. This is in fairly good agreement with cocrystal structures of resolution 1.7 and 1.9 Å for 1abe and 1abf, respectively.

Other groups have also used the DREIDING FF for MD for glycoproteins (29).

Summarizing, a number of studies validate that our FF and charges should lead to reasonable binding sites and energies for sugar–protein complexes such as in the current study. Indeed, we report here that the calculated binding energies for various sugars to OmpA correlate well with experimental invasion assays.

APPLICATION OF HIERDOCK PROTOCOL TO SUGARS BINDING TO OMPA

Coarse-Grain Docking Ensemble

Starting with the crystal structure of OmpA, we removed the waters so that the volume of the receptor site will be explored more completely. The HierDock procedure was as follows:

1. *Sampling volume*. The docking site was not known for OmpA and hence the negative image of the entire receptor's molecular surface was mapped as shown in Figure 1 and filled with a set of overlapping spheres. A probe of 1.4 Å radius was used to generate a molecular surface with 5 dots/Å. Sphere clusters generated for the whole binding site using the program Sphgen, is shown in Figure 1.
2. *Defining regions for docking*. The sphere filled volume from step1 representing the possible binding sites was partitioned into 12 regions. These regions included the 4 loops, the space in between the loops, and the space inside the barrel until halfway within the transmembrane region. Because the barrel is narrow and the ligands are reasonably big, it seemed improbable that the ligand would go deep into the barrel without any steric clashes. Moreover, the sugars are attached to Ecgp, the glycoprotein on the BMEC surface that will further prevent it from going far into the barrel cavity. Also, the barrel has internal polar networks that form a prominent barrier in the barrel interior with ordered water molecules inside the β-barrel.
3. *Ensemble selection (scoring).* To generate an ensemble of docked receptor–ligand complexes, we used the program DOCK (version 4.0) to sample various orientations and conformations of the ligands in the receptor site. We used the flexible ligand docking option in DOCK4.0, with torsion minimization of ligands. A non-distance-dependent dielectric constant of 1 and a distance cutoff of 10 Å were applied for calculating protein–ligand Coulombic interaction energy. The energy score in DOCK4.0 uses Coulombic energy and van der Waals energy as described in ref. 18. The conformations were ranked using energy scoring in DOCK4.0. The top 10–30 conformations were selected by energy score for each ligand in each of the 12 potential binding regions. These selected conformations were further used for fine-grain MD calculations.

Fine-Grain MD Search

The next step in HierDock is to perform a fine-grain MD with an all-atom force field to optimize the ligand conformation inside the binding pocket.

1. *Annealing MD.* For each of the 12 regions, the 20 best-scoring docked conformations from DOCK were subjected to five cycles of annealing dynamics (each from 50–600 K and back to 50 K with 25 ps of MD at each temperature). This allows for the optimization of the ligand conformation in the protein. One lowest-energy conformation is stored from each cycle of anneal-

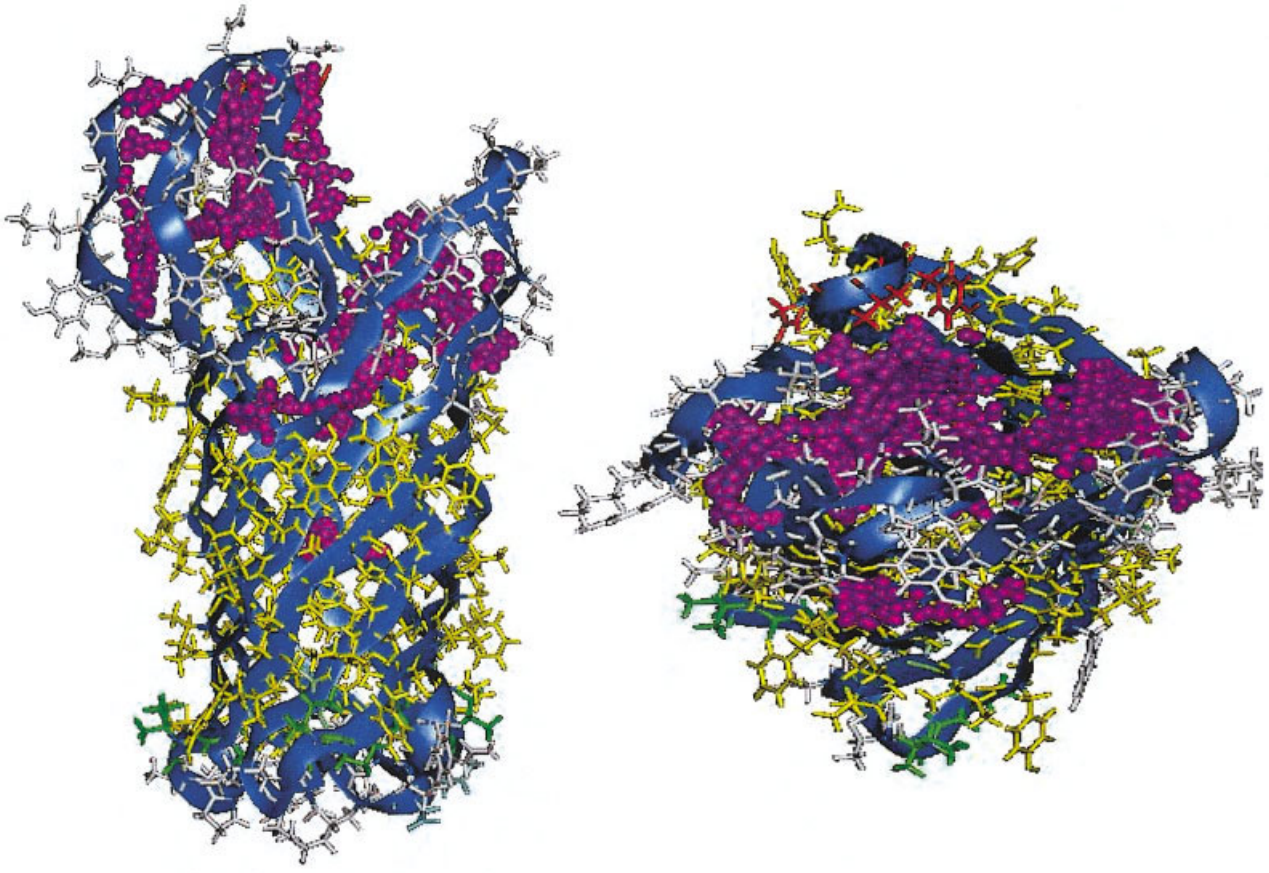

Fig. 1. Sphere-filled volume representing the possible binding sites on OmpA.

ing MD. The energies of the best-annealed structures were calculated using the all-atom DRIEDING force field[23] and SGB continuum solvation model. We find that this step of ligand optimization is critical in getting energetically favorable conformations for the complex (protein plus ligand).

2. *Binding energy calculation*. The binding energies of the 20×5 annealed structures for each ligand in each of the 12 docking regions were calculated. Binding energies were calculated using the DREIDING force field and charge equilibration[24] charges using MPSim simulation code.[19] Solvation effects for ligand binding were calculated using the SGB description of the continuum solvent model. The binding energy is calculated as the difference between the total energies of the complex (protein + ligand) and the sum of the protein and ligand energies. The best conformation from this pool was selected by the binding energy for each of the 12 docking regions.

Summarizing, the HierDock protocol uses a hierarchical strategy for conformation search and a corresponding scoring function to select a subset of structures for the next level. The coarse-grain level (DOCK4.0) uses a crude scoring function including just Coulombic and van der Waals interactions of the ligand with the protein. Using this scoring function, a subset of conformations generated by DOCK4.0 is selected for the annealing step. At the fine-grain level (annealing MD level), the scoring function uses an all-atom force field and continuum solvation method to calculate the binding energies and select the best-bound structure of the ligand in the protein.

Selection of the Best Two Regions Through Application to Chitobiose

A complete scanning of all possible docking regions for OmpA was done with chitobiose. The structure of the ligands used is shown in Figure 2. The final 1200 structures in 12 regions (100 conformations from each region) were scored using SGB solvation and the DREIDING force field. Comparison of the binding energies in various regions showed that regions 1 and 2 shown in Figure 3 have the best binding energies. Hence, these two regions were ranked as possible binding sites. The binding energy of conformations of chitobiose in regions 1 and 2 were about -15 and -20 kcal/mol, respectively, the difference of 5 kcal/mol being small enough to treat these two regions on an equal footing. Hence, these two regions were kept as possible binding regions for chitobiose. The binding energy of chitobiose in other regions was less than -5 kcal/mol and hence considered insignificant compared to regions 1 and 2.

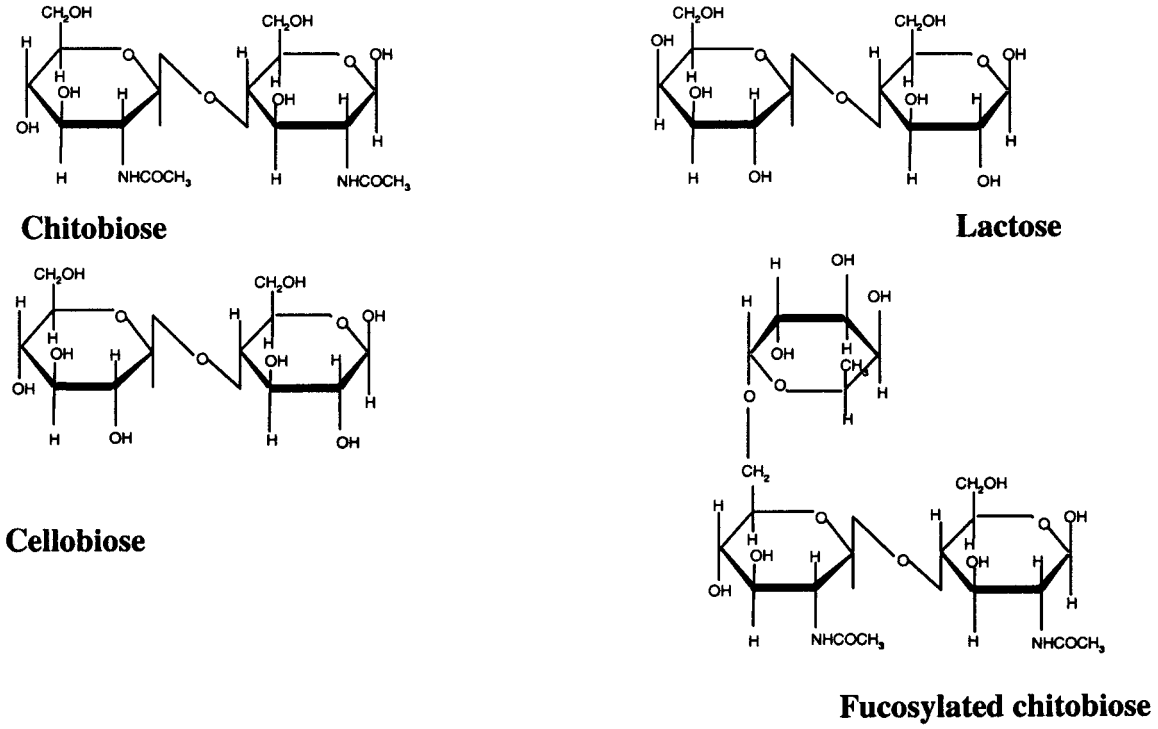

Fig. 2. Sugars used for docking in the 12 regions of OmpA.

Application to All Four Ligands

Having identified the probable binding sites for chitobiose, we then carried out the complete sequence of HierDock calculations over regions 1 and 2 for the three ligands using the structure of the ligands shown in Figure 2.

- Fucosylated chitobiose.
- Cellobiose.
- Lactose.

Thus, these ligands were docked and the structures were further annealed using MD and all the resulting complexes (OmpA + ligand) were optimized (energy minimized) using the conjugate gradient method. Finally, the binding energies of these ligands were calculated and ranked in these two binding sites.

Optimization with the Flexible Binding Site on OmpA

Protein flexibility is critical to determining the binding conformation and the critical ligand–protein interaction energies. Hence, we performed five cycles of 50 ps annealing MD heating from 50–600 K and cooling from 600 to 50 K for the best conformation of chitobiose bound to region 2. These simulations were performed allowing the ligand and all the amino acid residues that are in the top half of the barrel in Figure 3 to be flexible but keeping the rest of the protein fixed. These simulations optimized the hydrogen bonds and van der Waals contacts made by the ligand to particular residues in the binding cavity. The final conformation from these simulations was used for all analysis.

RESULTS AND DISCUSSION

Using the procedure described above, we predicted the binding site and energies of sugars in OmpA. Regions 1 and 2 shown in Figure 3 were ranked as the most favorable for binding of the best ligand (chitobiose) in OmpA. The binding energy of the best conformation of chitobiose is −15.42 kcal/mol in region 1 and −20.50 kcal/mol in region 2. In contrast, the calculated binding energy of chitobiose in all other regions was worse than −5.0 kcal/mol. Hence, we consider regions 1 and 2 as likely binding sites for chitobiose in OmpA. Indeed, peptides from region 1 [between external loop structures loop1 (L1) and loop2 (L2)] have been tested experimentally for inhibition of *E. coli* invasion.

The binding energies of chitobiose, fucosylated chitobiose, lactose, and cellobiose in regions 1 and 2 are shown in Figure 4. The result is that chitobiose has the best binding energy in both regions 1 and 2. This indicates that binding of chitobiose in these two regions of OmpA is specific. Experimentally, chitobiose dramatically reduced invasion (> 95%) when BMECs are infected with *E. coli* K1 after pretreating with chitobiose,[5] while none of the other ligands show reduced invasion. Thus, we find a good correlation between the binding energies of the ligands to OmpA and the experimental invasion assay measurements. This suggests that binding to OmpA may be a necessary step in the pathogenesis of bacterial meningitis.

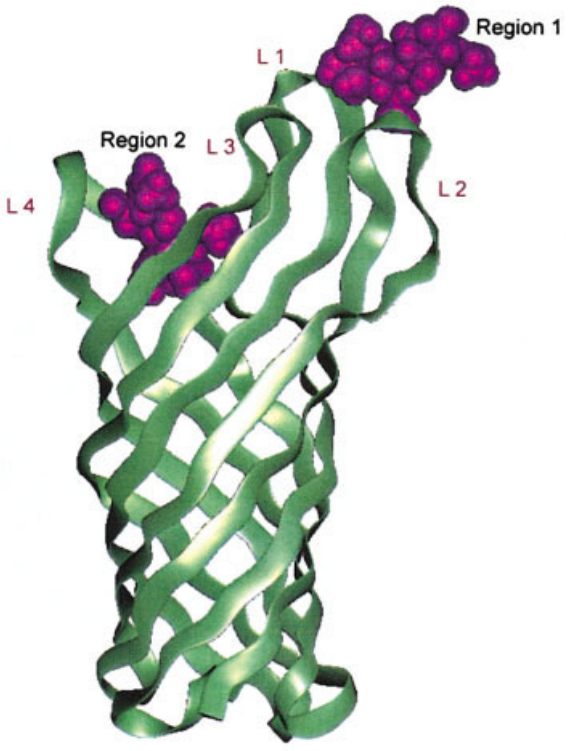

Fig. 3. OmpA regions 1 and 2. Region 1 (weaker binding) is between loops L1 and L2. Region 2 (stronger binding) is in the water-filled cavity between the 4 loops.

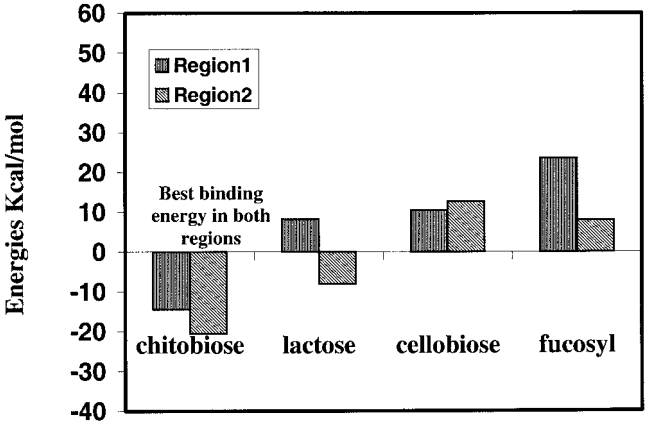

Fig. 4. Binding energies of the four ligands in regions 1 and 2. Chitobiose has the best binding energy in both regions.

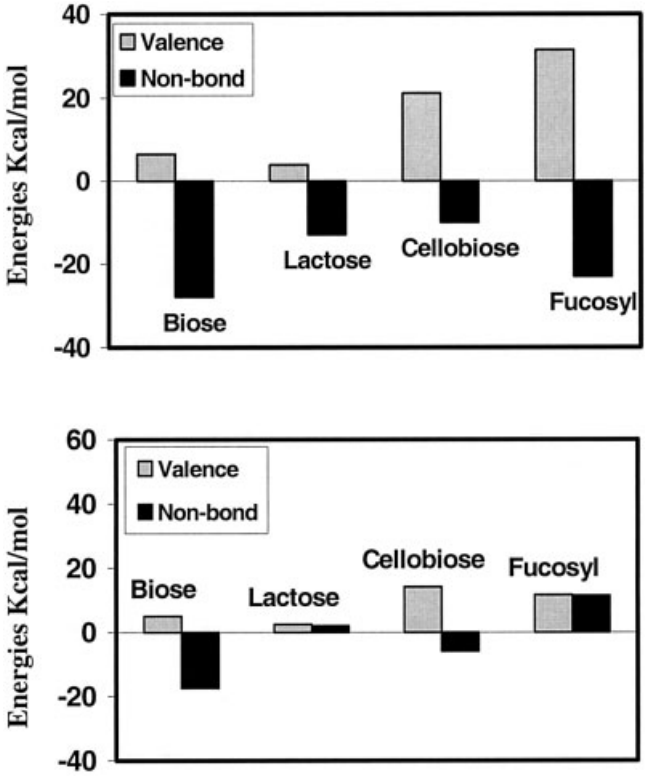

Fig. 5. Valence and nonbond energy contributions to the binding energy of lactose, chitobiose, cellobiose, and fucosylated chitobiose in (**a**) region 1 and (**b**) region 2.

Figure 5 shows the contribution of the valence and nonbond energies to the binding energy. Interestingly, lactose and cellobiose (both similar in size to chitobiose) do *not* show good binding energies. We attribute the lack of good binding energy for lactose compared to chitobiose to the absence of the $NHCOCH_3$ group. The hydrogen bonds made by the $NHCOCH_3$ group in chitobiose to His152, His20, and Arg157 are absent in lactose and cellobiose. On the other hand, fucosyl-substituted chitobiose in region 1 has nonbond interactions similar to chitobiose but the binding is weakened by the steric clash with the bulky fucosyl substitution. In region 2, fucosyl chitobiose does not have favorable nonbond interactions because it loses hydrogen bonds to His152 and Arg157.

Fucosyl chitobiose is a bulky ligand that does not bind to OmpA due to steric hindrance from the protein. We observed that during the annealing MD of the HierDock protocol (i.e., the ligand annealing MD for fucosyl chitobiose with OmpA fixed in region 2) the sugar ring was forced into a boat conformation due to steric clashes with the fixed protein. We found that the ligand gets trapped in this conformation during the cooling phase of annealing MD, resulting in a strained state for fucosyl chitobiose. Such a transformation to the boat form does not occur if annealing MD is performed with *all* protein atoms allowed to move along with the ligand. However, even with full relaxation (to the chair form), the binding energy of fucosyl chitobiose is still worse than chitobiose by 14.2 kcal/mol. We consider that annealing MD with all atoms movable is too expensive computationally to do for all docked structures. Thus, we refined the HierDock procedure to identify the large strain energies (caused in this case by the chair to boat transformation) in the internal energy of the ligand during protein-fixed annealing MD. Then, for structures leading to high internal strain energy the HierDock procedure now carries out annealing MD with all protein atoms movable when calculating the binding energy.

Chitobiose makes a number of critical contacts with residues on the loops in regions 1 and 2. In region 1, it makes significant contacts with residues Val68, Ser67,

TABLE I. Residues are in Binding Regions 1 and 2 of Chitobiose[†]

	Loop 1	Loop 2	Loop 3	Loop 4	Barrel
Region 1	Ile25 Asn26 **Asn27 Asn28** Gly29 Pro30	Ser67 Val68 Glu69			
Region 2	Gln18 Tyr19 His29 **Asp21** Thr22 Gly23 Leu24 Ile25 **His20**		Gly100 Met101 Val102 Trp103 Arg104 **Ala105** Asn115 His116 **Asp117** Thr118	Thr145 Asn146 **Asn147** Ile148 Gly149 Asp150 Ala151 **His152** Thr153 Ile154 Gly155 Thr156 **Arg157** Pro158 **Asp159** Asn160 Gly161	Asp106 Thr107 Tyr108 Ser109 Lys114

[†]Residues listed here are within 5 Å of chitobiose in regions 1 and 2. Residues in bold are within 3 Å of chitobiose and make critical contacts with chitobiose.

and Glu69 on loop L2 and with Asn27, Asn28, and Ile25 on loop L1 (Table I). The NHCOCH3 group on chitobiose makes a critical hydrogen bond with Asn27 as shown in Figure 6(a). There is experimental support of a role for residues in region 1. A number of peptides have been tested experimentally for inhibition of *E. coli* invasion, but only peptides from L1 and L2 were able to block invasion when compared against random peptides. This correlates well with our predicted site in region 1.

Region 2 is in the water-filled pocket between the extracellular loops. Chitobiose makes a number of contacts in this region, including a number of van der Waals contacts with loops L1, L3, and L4 and with some residues in the β-barrel. The residues that are within 5 Å of chitobiose are listed in Table I. Chitobiose is partially buried in the cavity between the loops (Table I) and present in the boundary between the β-barrel and the loops. Chitobiose makes electrostatic contacts with Trp103, Arg157, and His152 [shown in Fig. 6(b)]. On annealing MD with the protein cavity movable, the loops come closer to complex more strongly with the ligand. Loops 1 and 4 show maximum displacements from the original crystal structure (Fig. 7). Annealing dynamics suggest that chitobiose stays at the mouth of the cavity rather than going far into the cavity. OmpA has a narrow pore, which hinders chitobiose from inserting further into the cavity. We suggest experimental studies on invasion assays using the peptides from the list of residues in Table I.

In this study, we correlated the binding energies to the percentage invasion results from invasion assay experiments. It should be noted that many other steps might be involved in the pathogenesis leading to invasion of BMEC by *E. coli*. The correlation between the calculated binding energies and invasion assay results suggests that the binding of OmpA is a necessary step in the pathogenesis. Of course, there may be many other important factors. To further validate this model, we suggest several experimental tests of the predictions made by the model:

1. Synthesize peptides from binding region 2 on OmpA and test the efficacy of these peptides for blocking of *E. coli* invasion. For example, we recommend testing the following peptides for blocking invasion: QYHDTGLIH, QYHDT, HDTGL, TGLIH, DTGLI, GMVWRADTWS, GMVWR, ADTWS, VWRAD, KNHDT, NHDT, TNNIGDAHTIGTRPDNG, TNNIG, DAHTI, GTRPDNG, NIGDAHTIGTRPD, TRPDNG, NNIGDAHT, and AHTIGTRPDN.
2. Carry out point mutation studies for OmpA, targeting the polar and charged residues within 3 Å of chitobiose in region 2. Our predicted binding site suggests that mutations of residues Asp117, Asn147, His152, Arg157, and Asp159 will lead to disruption of OmpA interaction with chitobiose.
3. Design small-molecule drugs that would bind more strongly than chitobiose to regions 1 and 2 to inhibit the OmpA invasion of BMEC. We are currently using the data from our predicted sites to search for new compounds for experimental tests.

The glycoprotein (Ecgp) that interacts with OmpA has been sequenced and its two glycosylation sites have been identified recently by Prasadarao et al. (unpublished results). Based on these modeling studies, we propose two possible mechanisms of OmpA binding to the sugars in Ecgp:

- One possibility is a two-step mechanism: Here, the chitobiose is first recognized by the loop1 in region 1 and then transferred to region 2 for stronger binding. In this case, it seems plausible that region 1 is a recognition region and region 2 is the binding region. This recognition mode involving a sequence of two interaction regions has been shown for such other membrane proteins as CCR5,[30] a cofactor of CD4 in HIV invasion.
- A second plausible mechanism is that two sugar moieties from two glycosylated sites from Ecgp interact with both sites of OmpA at the same time. This might give stronger binding constants and additional selectivity.

CONCLUSIONS

We find two regions on OmpA that are potential interaction sites for GlcNAcβ1-4GlcNAc epitopes on glycoproteins

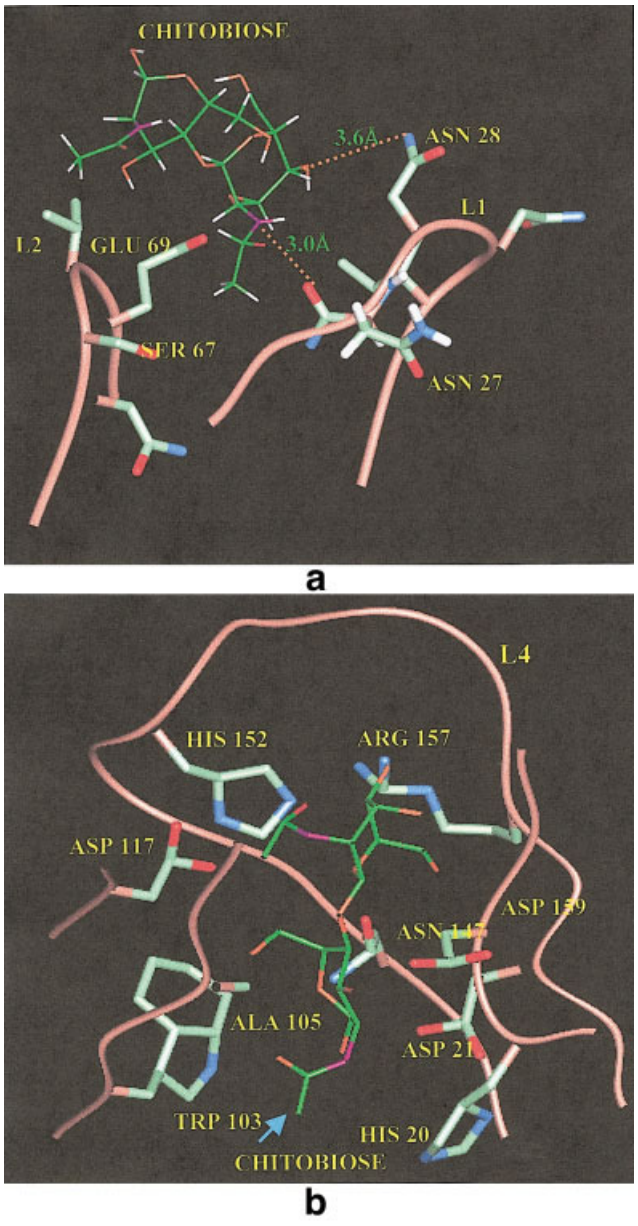

Fig. 6. (**a**) Important residues within 5 Å of chitobiose in region 1 (between loops L1 and L2). (**b**) Residues within 3 Å of chitobiose in region 2. Residues on loop 4 (which moves significantly) make important contacts with chitobiose. Most residues within 3 Å of chitobiose are either polar or charged.

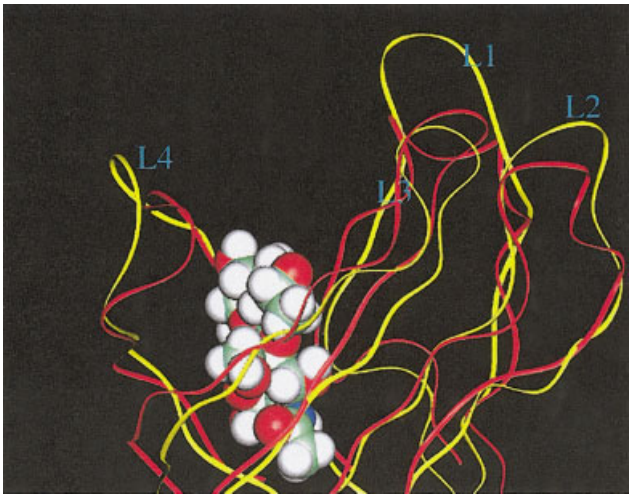

Fig. 7. Four loops move significantly on binding to chitobiose. Loops 4 and 1 show maximum change in structure.

of BMEC. For both regions, we showed that OmpA of *E. coli* binds most favorably to chitobiose as compared to cellobiose, fucosyl-substituted chitobiose, and lactose. The difference in the binding energies of OmpA with chitobiose and fucosylated chitobiose is of significance in understanding the pathogenesis of *E. coli* meningitis. Because most of the systemic cells of the body have fucosylated glycoproteins, this explains the specificity of *E. coli* invasion of BMEC. A good binding between OmpA and chitobiose arises from specific interactions of the NHCOCH3 groups on chitobiose with the OmpA residues. Lactose and cellobiose, although they have the same β1–4 linkage as chitobiose, lack the NHCOCH3 group, which is important in making favorable specific interactions. Fucosylated chitobiose, on the other hand, makes good contacts with the receptor and has a high nonbonded energy but it has an unfavorable valence energy.

The binding site predictions made in this article are testable either by point mutation studies or invasion assays. It is important to note that we studied the interaction of only sugars with OmpA because the experimental invasion assays were tested with the same sugars. We have not yet examined the effect of the glycoprotein, Ecgp, on this interaction. We intend later to include in our studies parts of Ecgp near its glycosylation sites.

ACKNOWLEDGMENTS

This work was supported by NIH/NICHD (W.A.G.) and NIH R29AI40567 (N.V.P.). The facilities of the Materials and Process Simulation Center used in this project are supported also by DOE (ASCI ASAP), NSF (CHE and MRI), NIH, ARO-MURI, Chevron Corp., MMM, Beckman Institute, Seiko-Epson, Avery-Dennison Corp., Asahi Chemical, General Motors, and Kellogg's.

REFERENCES

1. Gladstone IM, Ehrenkranz RA, Edbergt SC, Baltimore RS. A ten-year review of neonatal sepsis and comparison with the previous fifty-year experience. Pedriatr Infect Dis J 1990;9:819–825.
2. Klein JO, Feigin RD, McCracken GH Jr. Report of the Task Force on Diagnosis and Management of Meningitis. Pediatrics 1986; 78(suppl):959–982.
3. Unhanand M, Mustafa MM, McCracken GH, Nelson JD. Gram-negative enteric bacillary meningitis: a twenty-one-year experience. J Pediatr 1993;122:15–21.
4. Prasadarao NV, Wass CA, Weiser JN, Stins, Huang MFSH, Kim KS. Outer membrane protein A of Escherichia coli contributes to invasion of brain microvascular endothelial cells. Infect Immunol 1996;64:146–153.
5. Prasadarao NV, Wass CA, Kim KS. Endothelial cell GlcNAc beta 1-4GlcNAc epitopes for outer membrane protein A enhance traversal of Escherichia coli across the blood-brain barrier. Infect Immunol 1996;64:154–160.
6. Prasadarao NV, Wass CA, Kim KS. Identification and character-

ization of S fimbria-binding sialoglycoproteins on brain microvascular endothelial cells. Infect Immunol 1997;65:2852–2860.
7. Prasadarao NV, Wass CA, Stins MF, Shimada H, Kim KS. Outer membrane protein A-promoted actin condensation of brain microvascular endothelial cells is required for Escherichia coli invasion. Infect Immunol 1999;67:5775–5783.
8. Isberg RR. Discrimination between intracellular uptake and surface adhesion of bacterial pathogens. Science 1991;252:934–938.
9. Kindberg GM, Magnusson S, Berg T, Smedsrod B. Receptor-mediated endocytosis of ovalbumin by two carbohydrate-specific receptors in rat liver cells. The intracellular transport of ovalbumin to lysosomes is faster in liver endothelial cells than in parenchymal cells. Biochem J 1990;270:197–203.
10. Lecuit M, Dramsi S, Gottardi C, Fedor-Chaiken M, Gumbiner B, Cossart P. A single amino acid in E-cadherin responsible for host specificity towards the human pathogen Listeria monocytogenes. EMBO J 1999;18 3956–3963.
11. Pautsch A, Schulz GE. Structure of the outer membrane protein A transmembrane domain. Nat Struct Biol 1998;5:1013–1017.
12. Pautsch A, Schulz GE. High-resolution structure of the OmpA membrane domain. J Mol Biol 2000;298:273–282.
13. Floriano WB, Vaidehi N, Singer MS, Shepherd GM, Goddard WA III. Molecular mechanisms underlying differential odor responses of a mouse olfactory receptor. Proc Natl Acad Sci USA 2000;97: 10712 –10716.
14. Orozco R, Luque FJ. Theoretical methods for the description of the solvent effect in biomolecular systems. Chem Rev 2000;100:4187–4225
15. Kuntz ID, Blaney JM, Oatley SJ, Langridge R, Ferrin TE. A geometric approach to macromolecule–ligand interactions. J Mol Biol 1982;161:269–288.
16. Morris GM, Goodsell DS, Halliday RS, Huey R, Hart WE, Belew RK, Olson AJ. Automated docking using a Lamarckian genetic algorithm and an empirical binding free energy function. J Comput Chem 1988;19:1639–1662.
17. Wang P, Vaidehi N, Tirrell DA, Goddad WA III. Virtual screening for binding of phenylalanine analogs to phenylalanyl-tRNA synthetase. J Am Chem Soc. Forthcoming.
18. Ewing TA, Kuntz ID. Critical evaluation of search algorithms for automated molecular docking and database screening. J Comput Chem 1997;18:1175–1189.
19. Lim KT, Brunett S, Iotov M, McClurg B, Vaidehi N, Dasgupta S, Taylor S, Goddard WA III. Molecular dynamics for very large systems on massively parallel computers: the MPSim program. J Comput Chem 1997;18:501–521.
20. Tannor DJ, Marten B, Murphy R, Friesner RA, Sitkoff D, Nicholls A, Ringnalda MN, Goddard WA III, Honig B. Accurate first principles calculation of molecular charge distributions and solvation energies from ab initio quantum mechanics and continuum dielectric theory. J Am Chem Soc 1994;116:11875–11882.
21. Ghosh A, Rapp CS, Friesner RA. Generalized born model based on a surface integral formulation. J Phys Chem B 1998:102, 10983–10990.
22. Tang Y, Ghiralando G, Vaidehi N, Kua J, Mainz DA, Degrado WA, Goddard WA III, Tirrell DA. Stabilization of coiled-coil peptide domains by introduction of trifluoroleucine. Biochemistry 2001;40: 2790–2796.
23. Mayo SL, Olafson BD, Goddard WA III. DREIDING: a generic force field for molecular simulations. J Phys Chem 1990;94:8897–8909.
24. MacKerell AD, Bashford D, Bellott M, Dunbrack RL, Evanseck JD, Field MJ, Fischer S, Gao J, Guo H, Ha S, Joseph-McCarthy D, Kuchnir L, Kuczera K, Lau FTK, Mattos C, Michnick S, Ngo T, Nguyen DT, Prodhom B, Reiher WE, Roux B, Schlenkrich M, Smith JC, Stote R, Straub J, Watanabe M, Wiorkiewicz-Kuczera J, Yin D, Karplus M. All-atom empirical potential for molecular modeling and dynamics studies of proteins. J Phys Chem B 1998;102:3586–3616 .
25. Rappé AK, Goddard WA III. Charge equilibration for molecular dynamics simulations. J Phys Chem 1991;95:3358–3363.
26. Brameld KA Goddard WA III. Substrate distortion to a boat conformation at subsite-1 is critical in the mechanism of family 18 chitinases. J Am Chem Soc 1998;120:3571–3580.
27. Brameld KA Goddard WA III. The role of enzyme distortion in the single displacement mechanism of family 19 chitinases. J Am Chem Soc 1998;95:4276–4281.
28. Floriano WB, Vaidehi N, Goddard WA III. Virtual ligand screening of large molecule databases with a hierarchical docking protocol. In preparation.
29. Gabriel JL, Mitchell WM. Proposed atomic structure of a truncated human immunodeficiency virus glycoprotein gp120 derived by molecular modeling: target CD4 recognition and docking mechanism. Proc Natl Acad Sci USA 1993;90:4186–4190.
30. Yang J, Zhang YW, Huang JF, Zhang YP, Liu CQ. Structure analysis of CCR5 from human and primates. Theo Chem 2000;505: 199–210.